



Published in final edited form as:

Sci Transl Med. 2009 December 16; 1(11): 11ra22. doi:10.1126/scitranslmed.3000397.

Synthetic Platelets: Nanotechnology to Halt Bleeding

James P. Bertram¹, Cicely A. Williams², Rebecca Robinson¹, Steven S. Segal³, Nolan T. Flynn⁴, and Erin B. Lavik^{5,*}

¹Department of Biomedical Engineering, Yale University, 55 Prospect Street, Malone Engineering Center, New Haven, CT 06511

²Interdepartmental Neuroscience Program, Yale University, New Haven, CT, 06511

³Department of Medical Pharmacology and Physiology, University of Missouri School of Medicine, Columbia, MO 65212 & Dalton Cardiovascular Research Center, Columbia, MO 65211

⁴Department of Chemistry, Wellesley College, Wellesley, MA 02481

⁵Department of Biomedical Engineering, Case Western Reserve University, Cleveland, OH 44106

Abstract

Blood loss is the major cause of death in both civilian and battlefield traumas. Methods to staunch bleeding include pressure dressings and absorbent materials. For example, Quik-clot effectively halts bleeding by absorbing large quantities of fluid and concentrating platelets to augment clotting, but these treatments are limited to compressible and exposed wounds. An ideal treatment would halt bleeding only at the injury site, be stable at room temperature, be administered easily, and work effectively for internal injuries. We have developed synthetic platelets, based on Arg-Gly-Asp functionalized nanoparticles, that halve bleeding time after intravenous administration in a rat model of major trauma. The effects of these synthetic platelets surpass other treatments including recombinant factor VIIa, which is used clinically for uncontrolled bleeding. Synthetic platelets were cleared within 24 hours at a dose of 20 mg/ml, and no complications were seen out to 7 days after infusion, the longest time point studied. These synthetic platelets may be useful for early intervention in trauma and demonstrate the role that nanotechnology can have in addressing unmet medical needs.

Keywords

PLGA; nanoparticles; PEG; hemostasis; coagulation cascade; trauma

*Prof. E.B. Lavik, Department of Biomedical Engineering, Case Western Reserve University, Room 309 Wickenden Building, 10900 Euclid Avenue Cleveland, OH 44106-7207, erin.lavik@case.edu .

Author contributions: J.P.B. designed and performed experiments, analyzed results, and wrote the paper. C.A.W., R.R., and N.T.F. assisted in performing experiments and provided edits for the paper. S.S.S. provided expertise and training in vascular injury techniques and analysis and provided edits for the paper. E.B.L. designed the approach and experiments, provided funding, assisted in analysis of results, and edited the paper.

Competing interests: Bertram and Lavik are inventors on a filed patent regarding this work.

Accession numbers: None.

Supplementary Material

Fig. S1. Polymer synthesis and characterization.

Fig. S2. Polymer characterization and in vitro assay with collagen.

Fig. S3. In vitro analysis of PRP with synthetic platelets.

Fig. S4. In vivo analysis of bleed times for different concentrations of synthetic platelets.

Introduction

Traumatic injury is the leading cause of death for individuals between the ages of 5 and 44 (1), and blood loss is the major factor in both civilian and battlefield trauma (2,3). After injury, the cessation of bleeding, or hemostasis, is established through a series of coagulatory events including platelet activation. With severe injuries, however, these processes are insufficient and uncontrolled bleeding results. Although immediate intervention is one of the most effective means of minimizing mortality associated with severe trauma (4), pressure dressings and absorbents are currently the only hemostats available for field administration.

Alternatives to topical dressings include allogeneic platelet transfusions, clotting factors, and platelet substitutes, but limited efficacy, immunogenicity, and thrombosis have stalled their application (5). Administration of allogeneic platelets can halt bleeding. However, platelets have a short shelf life, and administration of allogeneic platelets can cause graft versus host disease, alloimmunization, and transfusion-associated lung injuries (6). Recombinant factors including activated factor VII (NovoSeven) can augment hemostasis, but immunogenic and thromboembolic complications are unavoidable risks (7). Nonetheless, NovoSeven is used in trauma and surgical situations where bleeding cannot otherwise be controlled (8). Non-platelet alternative coagulants including red blood cells modified with the Arg-Gly-Asp (RGD) sequence, fibrinogen-coated albumin microcapsules, and liposomal systems have been studied as coagulants (9), but toxicity, thrombosis, and limited efficacy restrict the clinical utility of these products (5).

Polymer engineering has opened up new possibilities for controlling bleeding. For example, a self assembling peptide rapidly halts bleeding in a number of injury models when applied topically (10), and a block copolymer of hemoglobin and fibrinogen acts as an oxygen carrier and maintains normal bleeding times at high concentrations where typical oxygen carriers lead to hemodilution and long bleeding times (11). We have taken a different approach and have designed synthetic platelets based on functionalized nanoparticles that bind to activated platelets to augment clotting in a safe, localized manner. This system leverages existing biological processes by providing a nanostructure that binds to activated platelets and enhances their rate of aggregation, which stops bleeding. They are made from polymers that are already used in the medical device and pharmaceutical industries, and a strong track record of safety makes them well suited for clinical translation.

We tested the synthetic platelets *in vitro* to optimize their binding efficiency to activated platelets and *in vivo* in a rat major femoral artery injury model to determine their efficacy in promoting hemostasis and their biodistribution. The synthetic platelets halved bleeding time after intravenous administration in the femoral artery injury model and performed significantly better than activated recombinant factor VII (rFVIIa), which is currently being used in the clinic for uncontrolled bleeding.

Results

Design and synthesis of synthetic platelets

Our synthetic platelets consist of poly(lactic-co-glycolic acid)-poly-L-lysine (PLGA-PLL) block copolymer cores to which we conjugated polyethylene glycol (PEG) arms terminated with RGD functionalities (Fig. 1A). ¹H-NMR demonstrated successful conjugation of PEG to PLGA-PLL (Fig. S1C). Nanospheres were fabricated with a single emulsion solvent evaporation technique (12), which resulted in core diameters of approximately 170 nm by scanning electron microscopy (SEM) (Fig. 1B, D). After fabrication, nanospheres were analyzed with ¹H-NMR to confirm that the conjugated PEG was present. The subsequent

conjugation of RGD to PLGA-PLL-PEG nanospheres was then confirmed with amino acid analysis (Fig. 1C). Amino acid analysis was also employed for ascertaining the RGD conjugation for the PLGA-PLL-PEG-RGD polymer used for in vitro characterization (Fig. S2A). RGD conjugation efficiency was independent of both the PEG molecular weight and peptide sequence (i.e. RGD versus GRGDS) (Figs. 1C and S2A). Synthetic platelets have an average RGD peptide content of $3.3 \pm 1.1 \mu\text{mol/g}$ (mean \pm SD) (Fig. 1C), which corresponds to a conjugation efficiency of $16.2 \pm 5.9 \%$ (mean \pm SD) (~ 600 RGD moieties/synthetic platelet). The coupling agent used to attach the peptide, carbonyldiimidazole, CDI, is hydrolysable in water, and thus can be quenched during the aqueous peptide coupling leading to the modest efficiency. One could augment the efficiency by repeated activation and coupling reactions or the use of an alternative agent, but the efficiencies here were effective in our subsequent studies. Although cores are approximately 170 nm in diameter for all of the preparations (Fig. 1D), the hydrodynamic diameter of the spheres, determined by dynamic light scattering (DLS), increased with increasing PEG molecular weight (Fig. 1D). The SEM and DLS results suggest that a surface enrichment of PEG arms exists, and in a hydrated environment PEG arms extend to create a PEG corona on the nanosphere surface (13). On the basis of these results, we concluded that under hydrated conditions, the surface proximity of the conjugated RGD peptide varies as a function of PEG molecular weight.

In vitro validation and optimization of synthetic platelets

The surface proximity of the RGD functionality affects interactions with activated platelets (14). To determine the optimal PEG arm length, as well as to identify the most appropriate peptide sequence, we adapted an in vitro platelet aggregation and adhesion assay (Fig. 2A) (14). The in vitro assay provided a simple means to assess the role of the components of the synthetic platelets on platelet adhesion and aggregation. Other traditional in vitro assays such as the aggregometer could not be used with our synthetic platelets because the nanoparticles led to substantial scattering in the system which produced noise that masked the results. The in vitro platelet aggregation and adhesion assay was validated with collagen controls (Fig. S2B). We coated the surface of a 96-well plate with variants of the PLGA-PLL-PEG-RGD polymer (Fig. S1A). Using 5-chloromethylfluorescein diacetate (CMFDA)-labeled platelets and the aggregation stimulant adenosine diphosphate (ADP), we examined the effects of the PEG length and RGD functionality on platelet aggregation and adhesion (Fig. 2B-C). Platelet aggregation increased with increased PEG length, with PEG 4600 compounds leading to greater adhesion and aggregation than PEG 1500 compounds for all RGD variants studied. This is consistent with previous observations (15).

We found that activated platelet adhesion increased as we added flanking amino acids around the RGD sequence, with the GRGDS formulations leading to the greatest adhesion (Fig. 2D). Control experiments verified that PEG alone, and the conservative substitute peptide, 4600-GRADSP, yielded the same values as the PLGA-only group, inducing only minimal adhesion and aggregation.

For clinical utility, it is critical that the activated platelets bind specifically to the synthetic platelets, as nonspecific binding or induced platelet activation could lead to adverse concomitant thrombotic events, including embolism and stroke. We found that non-activated platelets did not bind to any of the PLGA-PLL-PEG-RGD polymers tested (Fig. S3C). Furthermore, platelets did not activate without the addition of ADP. In fact, the polymers did not induce platelet adhesion, even with agitation, except when ADP was added (Fig. S3D). As a simple test of our system, we added synthetic platelets to platelet-rich plasma (PRP) (Fig S3). Even with prolonged agitation (10 minutes), synthetic platelets do not induce endogenous platelet aggregation. This is in contrast to PRP added to the collagen-coated control wells. Even in the absence of ADP, endogenous platelets aggregated and adhered to the collagen (Fig. S2B). We only saw adhesion and coagulation with the synthetic platelets

when a proaggregatory stimulus (ADP) was added. The materials used to fabricate synthetic platelets do not activate endogenous platelets, and unactivated platelets do not bind, suggesting that the materials are unlikely to induce activation or non-specific platelet binding on their own.

In vivo: femoral artery injury model

The goal of this work was to develop a safe synthetic platelet with hemostatic efficacy in vivo. We tested our synthetic platelets in a rat model of a major femoral artery injury (Fig. 3A) (16). The injury leads to blood spurting in a continuous stream from the injury site (Fig. 3A) and is easily visualized. We investigated three doses, 10 mg/ml, 20 mg/ml, and 40 mg/ml of the synthetic platelets (Fig. S4A). We found that 10 mg/ml had no effect on bleeding time and 40 mg/ml produced cardiopulmonary complications in some animals presenting as elevated heart rate and gasping. Therefore, we focused on determining the optimal particle characteristics with intravenous administration at 20 mg/ml.

The PEG-1500 nanospheres with the GRGDS peptide led to the greatest reduction in bleeding time (Fig. 3B) paralleling the in vitro findings. Also paralleling the in vitro findings, was the fact that there was a greater reduction in bleeding time with the RGD functionalized PEG 4600 spheres as compared to their PEG 1500 counterparts (Fig. 3C). 4600-GRGDS nanospheres led to significantly shorter bleeding times than the 1500-GRGDS nanospheres (n=5, P<0.05).

The injury alone with no injection gave a baseline bleeding time of 240 ± 15 seconds (mean \pm SEM, n=5). Injection of the 4600-GRGDS synthetic platelets halved the bleeding time (131 ± 11 seconds (mean \pm SEM, n=5)) (Fig 3C). To validate our synthetic platelets as a hemostatic agent, we compared bleeding times following synthetic platelet administration to bleeding times after the injection of recombinant human factor VIIa (rFVIIa). rFVIIa has proven clinically useful in the treatment of surgery- and trauma- associated bleeding (17) and is the current standard of care for uncontrolled bleeding (8). Although a bolus injection of rFVIIa (100 μ g/kg) (the recommended dose is 90-100 μ g/kg) significantly reduced bleed times (187 ± 16 seconds (mean \pm SEM, n=5)), 4600-GRGDS synthetic platelets reduced bleeding time approximately 25% more than rFVIIa (Fig. 3C). Furthermore, 4600-GRGDS synthetic platelets stored in a lyophilized state at room temperature for 2 weeks, maintained their hemostatic properties with no reduction in efficacy (Fig 3D).

In these studies, the agents were administered intravenously prior to the injury. We chose this approach initially because the bleeding times in this injury without treatment (240 ± 15 seconds) are close to the time it took to inject the synthetic platelets or controls (180 seconds). However, for the synthetic platelets to be clinically effective, they need to work when administered after an injury. Therefore, we tested the synthetic platelets in the same rat femoral artery injury model, but we administered the synthetic platelets (20 mg/ml, 0.5 ml injected) or one of the controls over a period of 20 seconds. Administration of saline alone (0.5 ml) or the unfunctionalized PEG 4600 nanospheres (20 mg/ml, 0.5 ml administered) increased bleeding time as compared to the no injection control group. This is likely the result of systemic blood dilution due to the rapid bolus administration of fluid, a significant concern when administering fluids and clotting factors intravenously after injury (18). Nonetheless, even with this diluting effect, the 4600-GRGDS synthetic platelets significantly reducing bleeding time by approximately 23% compared to no injection, and 31% compared to saline injection (Fig. 3E).

Participation of synthetic platelets in the clot

We next determined whether synthetic platelets were present in the clots. We excised the injured vessel segments and performed scanning electron microscopy. Synthetic platelets were intimately associated with the fibrin mesh (Fig. 3F) and distributed throughout the clot on the luminal, interior surface of the femoral artery (Fig. S4B).

Biodistribution of synthetic platelets

For synthetic platelets to be therapeutically viable, they must be effectively cleared when not participating in clot formation at the site of injury. To test this parameter, synthetic platelets (4600-GRGDS) were labeled by encapsulating coumarin 6 (C6), a fluorochrome commonly used for biodistribution studies (19). We examined the biodistribution and clearance of C6-labeled synthetic platelets up to 7 days after intravenous injection using UV/Vis spectroscopy. Less than 0.5% of the C6 fluorochrome label was released from the nanospheres after 24 hours, and approximately 1.5% was released after 7 days (Fig. 4A), indicating that virtually all of the C6 fluorescence was associated with synthetic platelets. A characteristic distribution of synthetic platelets was observed consistent with intravenous nanosphere administration (Fig. 4B) (20). Within 5 minutes of injection, 68.3% of the injected particles were found in the liver, 16.1% were in the blood, and minimal accumulations were seen in the kidneys, lungs and spleen (< 3.6%, 2.2%, and 5.2%, respectively). The sensitivity of our biodistribution analysis is 0.2 ng of C6/mg of tissue and 3.3 ng of C6/ml of plasma. At 3 and 7 days after injection, no C6 was detected, suggesting that all synthetic platelets had been cleared from circulation. Furthermore, no adverse effects were seen in any of the animals, at all time points. We also examined the biodistribution of synthetic platelets immediately after a femoral artery injury, and 1 hour after injury (Fig. 4C and D). For both time points, tissue distribution was similar for the injured and uninjured animals (equivalent to 10 minutes and 1 hour time points in uninjured animals). This suggests that even following a severe injury and with circulating activated platelets, the unbound synthetic platelets are effectively cleared within 24 hours.

Quantification of synthetic platelets within the clot

We were able to both visualize and quantify the C6 labeled synthetic platelets in the clot following injury. Cross sections show the synthetic platelets (green) distributed throughout the clot (Fig. 5A), consistent with the SEM findings (Fig. 3F and Fig. S4B). We quantified the amount of synthetic platelets within the clots using HPLC and compared these findings to the distribution of C6-labeled PEG 4600 nanospheres with no variants on the RGD functionality. Although PEG 4600 nanospheres were entrapped in the clots following injury, clots from animals that received synthetic platelets had more than double the number of particles compared to PEG 4600 nanospheres [3.9 ± 0.4 and 1.8 ± 0.2 ng of C6, respectively (mean \pm SEM, $n=5$)] (Fig. 5B). However, PEG 4600 nanospheres had no significant effect on bleeding time (Fig. 3C), suggesting that the synthetic platelets interact preferentially with activated platelets due to RGD functionalization, and thereby actively halt bleeding (as opposed to indirectly inducing platelet flocculation).

Discussion

The ultimate goal of this work was to design and optimize a synthetic platelet that is stable at room temperature, safely administered intravenously and able to halt bleeding. Through our *in vitro* studies, we found that nanospheres functionalized with PEG arms with a molecular weight of 4600 Da and the GRGDS moiety led to the greatest platelet adhesion and aggregation. These trends were repeated *in vivo* in the rat femoral artery injury model.

It has been well established that the incorporation of the RGD moiety can influence cellular interactions with biomaterials (21), and the proximity of the moiety to the biomaterial surface is a critical parameter in these interactions (14,22). By having a longer PEG spacer between the PLGA surface and the RGD moiety, there is a greater probability that the RGD functionality is available to bind with the activated platelets. Beyond a certain PEG arm length, specifically a molecular weight of 5000 Da (13), the PEG molecule has enough repeat units to have a strong probability of folding over and shielding the functional region.

Activated platelets bind to RGD moieties through specific ligand-receptor interactions between RGD and surface receptors expressed on activated platelets (23). More specifically, RGD interacts with the activated platelet receptors GPIIb-IIIa and integrin $\alpha_v\beta_3$ (14). We hypothesize that the RGD moiety, and the GRGDS moiety in particular, interacts with the activated platelets through these receptors to promote adhesion between the polymers and the platelets. It has been shown previously that flanking amino acids to the RGD motif produce a more active binding conformation (24). This increased bioactivity in turn influences integrin affinity for the RGD moiety (25), and increases cellular attachment (15). These features explain why the GRGDS peptide demonstrates the greatest binding and adhesion of the activated platelets. Longer, more specific sequences have higher affinities for activated platelets than the GRGDS peptide. However, the length of the peptide can have dramatic effects on its temperature stability (26) as well as production costs. We designed these synthetic platelets to be stable at room temperature to facilitate their potential administration in the field. Therefore, we focused on short peptides for optimization of the platform.

Our results show that RGD-functionalized polymer interacts specifically with activated platelets. In the in vitro studies, the PEG alone and conservative substitute peptide, 4600-GRADSP, groups behaved like the PLGA-only group, inducing only minimal adhesion and aggregation. Thus, neither the polymer alone nor the polymer with a substitute peptide induces adhesion and aggregation, while adhesion and aggregation are seen with all of the specific RGD variants. This indicates that the activated platelets' affinity for the GRGDS moiety increases platelet adhesion to the polymer. This implies that the binding of activated platelets to the functionalized PLGA-PLL-PEG is specific. Similar findings have been reported with cell attachment assays for other cell types (22).

Non-functionalized nanoparticles can activate platelets and alter the coagulation cascade (27). It is hypothesized that the surface charge on the particles, their aggregation in water, and their shape are important parameters influencing platelet activation and potentially thrombus formation in vivo (27). Thus, it is important for safety to establish what impact the components of our synthetic platelets have on coagulation. The cores of the synthetic platelets are degradable polyester nanoparticles, and degradable polyester nanoparticles have been shown to induce clot formation (28). However, PEGylation of the particles reduces this effect dramatically. During normal clot formation, PEGylated nanoparticles do not alter clotting behavior (28). This lack of alteration in the coagulation cascade with PEGylated nanoparticles is attributed to the hydrophilic PEG corona which reduces the surface adsorption of plasma proteins and lipids. The PEG corona also acts as a shield for nanoparticles, increasing their circulation time (29) which allows the particles to reach the site of injury before being cleared.

Ease of administration, stability, non-immunogenicity, and hemostatic efficacy without pathological thrombogenicity are required properties of an intravenously administered hemostatic agent, and were critical design requirements of the synthetic platelets. Each of the materials used in our synthesis-- PLGA, PEG, and the RGD moiety-- have been approved in other devices by the FDA (30-32). The choice of PEGylated nanoparticles

facilitated the synthetic platelets' administration and residence in the circulation (33). By using a small, synthetic peptide sequence (RGD) rather than a protein, problems with immunogenicity and stability are minimized. Furthermore, the lower cost of smaller active peptide sequences makes them more amenable to translation than large protein counterparts. The track record of the materials and design for safety, coupled with lack of platelet activation and rapid clearance exhibited here, suggests that the synthetic platelets will be safe. The significant improvement in halting bleeding as compared to established treatments (rFVIIa) demonstrates that these novel synthetic platelets are a strong candidate for translation into not only the clinic, but also, a field medic's bag. These results provide compelling evidence that these synthetic platelets have the potential to stop bleeding and fundamentally change trauma care.

Materials and Methods

Materials

Poly(lactic-co-glycolic acid)(PLGA) 503H (Resomer 503H, 50:50 lactic to glycolic acid ratio and a $M_n \sim 25$ kDa) was from Boehringer Ingelheim. H signifies PLGA terminated with a carboxylic acid group. Poly(ϵ -carbobenzoxy-L-lysine) (molecular weight ~ 1000 Da) was from Sigma. Poly(ethylene glycol) (PEG)(molecular weight ~ 1500 and 4600 Da) was from Acros Organics and Sigma, respectively. Arg-Gly-Asp (RGD) peptide sequences were from EMD Biosciences. Peptide sequences include RGD, Arg-Gly-Asp-Ser (RGDS), Gly-Arg-Gly-Asp-Ser (GRGDS), and Gly-Arg-Ala-Asp-Ser-Pro (GRADSP). Collagen I (rat tail) was from BD Biosciences. Deuterated dimethyl sulfoxide (D_6 -DMSO) was from Cambridge Isotope Laboratories, Inc. Poly(vinyl alcohol) (PVA) (88 mol% hydrolyzed) was purchased from Polysciences. CMFDA (5-chloromethylfluorescein diacetate) was from Molecular Probes. Recombinant human factor VIIa (rFVIIa) was from Innovative Research. Vectashield with DAPI was from Vector Laboratories. All other chemicals were A.C.S. reagent grade and other materials were used as received from Sigma.

Methods

Polymer synthesis and characterization—Detailed methods are included in the supplementary material.

Nanosphere fabrication and characterization—Detailed methods are included in the supplementary material.

Fluorescent labeling of rat platelets—Detailed methods are included in the supplementary material.

Validation of in vitro assay—Detailed methods are included in the supplementary material.

In vitro characterization of PLGA-PLL-PEG-RGD polymer—Ninety-six well plates were coated with PLGA-PLL-PEG-RGD polymer to examine interactions between our polymers and platelets. Briefly, 5 mg of polymer was dissolved in 1.0 ml trifluoroethanol (TFE). One hundred microliters of polymer solution was added to each well of a 96-well plate. By allowing the TFE to evaporate, we were able to effectively coat the well with our polymer (³⁴). Wells were then washed three times with PBS. Following the PBS rinse, 100 μ l of PRP with CMFDA fluorescently labeled platelets (5×10^8 platelets/ml) was added to each well. This was followed by the addition of 10 μ l of 100 μ M ADP as a proaggregatory stimulus, or PBS as a control. Immediately following ADP/PBS addition, the 96-well plate was agitated for one minute on an orbital shaker (Barnstead International) at 180 rpm (14).

Following a 3 minute equilibration, plasma and non-aggregated platelets were gently extracted, and entire wells were imaged from the bottom with a 4x objective at 490nm / 525nm (excitation/emission) (Olympus IX71 Fluorescent microscope). Area of fluorescence was then quantified to elucidate the differences in platelet adherence/aggregation⁽³⁵⁾. Experiments were performed in triplicate.

Examination of synthetic platelets in vitro—For qualitative examination, a variation of the in vitro assay was employed. Instead of coating the well with polymer, synthetic platelets in PBS (10 μ l of 1500-RGDS synthetic platelets at 20 mg/ml) were added to wells containing PRP (100 μ l). This was followed by the addition of 10 μ l of 100 μ M ADP or PBS. Wells with PBS were agitated for up to 10 minutes, while wells with ADP were agitated for only 1 minute. Following agitation, wells were examined for opaque aggregates of endogenous/synthetic platelets. The wells were then photographed.

In vitro release of C6 from 4600-GRGDS nanospheres—The release of C6 from the 4600-GRGDS nanospheres was investigated. Briefly, 5 mg of C6 labeled 4600-GRGDS nanospheres were reconstituted with 1.0 ml of PBS in 1.5 ml Eppendorf tubes. Mixtures were then incubated at 37°C on a rotating shaker. At specific time points (1 hour and 5 hours and 1, 3, and 7 days), the mixture was centrifuged and the supernatant was collected. An equal volume of PBS was then added to replace the withdrawn supernatant and the nanospheres were resuspended and returned to the shaker. Extracted supernatants were freeze-dried and reconstituted in 1.0 ml DMSO. Samples were then analyzed at 444/538nm (excitation/emission) (SpectraMax M5 spectrophotometer, Molecular Devices) for C6 content. A C6 standard curve in DMSO was established with sensitivity to 10 ng/ml.

Surgical preparation for femoral artery injury—Male Sprague Dawley rats (~180-200g), obtained from Charles River Laboratories, were used in accordance with procedures approved by Animal Care and Use Committees of Yale University and follow the NIH Guide for the Care and Use of Laboratory Animals. Rats were initially anesthetized with an i.p. injection of ketamine/xylazine and placed in a supine position on a heat pad. Body temperature was maintained at 37°C. An incision was made from the abdomen to the knee on the left hindlimb. Following exposure of the femoral vein, polyethylene tubing (PE 10) was used as a catheter and inserted into the femoral vein. Sutures secured the catheter, the cavity was closed, and the skin was sutured. The cannulated vein was later used for the intravenous administration of anesthetics and treatment groups.

Following cannulation, a similar incision was made on the right hindlimb, and the femoral vessels were exposed. A portion of the femoral artery was then isolated from the surrounding connective tissue by placing a small piece of aluminum foil between the vessel and the underlying tissue. Once the vessel was isolated, the cavity was irrigated (5 ml/minute) with 0.9% NaCl irrigation fluid (Braun Medical Inc.) at 37°C. Following a 10 minute equilibration period, the synthetic platelets or control treatment was administered intravenously through the cannulated femoral vein over 3 minutes.

In vivo analysis of hemostasis—Male Sprague Dawley rats (~180-200g), obtained from Charles River Laboratories, were used in accordance with procedures approved by Animal Care and Use Committees of Yale University. Treatment groups included a sham (injury alone), vehicle (saline) alone, rFVIIa (100 μ g/kg), PLGA-PLL-PEG (unfunctionalized nanospheres) or PLGA-PLL-PEG-RGD nanospheres (synthetic platelets) at 20 mg/ml. All treatments (excluding sham group) were in 0.5 ml vehicle solution. The surgeon performing the injury was blinded to the treatment groups. Anaesthetized rats were given an intravenous injection via femoral vein cannula, and the synthetic platelets or control were allowed to circulate for 5 minutes. Following circulation, a thrombogenic

injury was induced in the femoral artery (16). Briefly, a transverse cut made with microscissors encompassing one-third of the vessel circumference resulted in the extravasation of blood. Time required for bleeding to cease for at least 10 seconds was recorded as the bleeding time. Experiments included five rats per group. See Supplementary information for surgical preparations.

Administration of synthetic platelets after injury—A variation to the described artery injury model included the intravenous administration of synthetic platelets immediately following injury. For post-injury injections, treatments [saline, PEG 4600 (20 mg/ml), or 4600-GRGDS (20 mg/ml)] were administered over a 20 second interval immediately following an injury to the femoral artery.

Biodistribution—RGD nanospheres were fabricated as described in the supplementary information, with the addition of C6 to the DCM (0.5% w/v). The biodistribution of the RGD nanospheres was examined after intravenous injection. A 0.5 ml injection (20 mg/ml) of C6 labeled PEG4600-GRGDS nanospheres was administered via tail vein injection. Biodistribution was examined at 5 minute, 10 minute, 1 hour, 1, 3, and 7 days post injection. At each time point, animals were euthanized and blood, lungs, liver, kidneys and spleen were collected. Blood was centrifuged (180 g for 10 minute), and 1.0 ml of plasma was extracted. Plasma and organs were then freeze-dried for 3 days and dry organ mass was then determined.

To determine organ C6 content, 50 mg of dry organ was homogenized (Precellys 24 Tissue homogenizer, Bertin Technologies) in 1.0 ml DMSO. The homogenates were covered and incubated at 37°C for 6 hours to ensure nanosphere/C6 dissolution. Homogenates were then centrifuged and 200 µl samples were extracted and analyzed for C6 content. Samples were analyzed at 444/538nm (excitation/emission) (SpectraMax M5 spectrophotometer, Molecular Devices) for C6 content. A C6 standard curve in DMSO was established with sensitivity to 0.2 ng/mg of tissue and 3.3 ng/ml of plasma. Organs without C6 were analyzed at the same wavelengths to establish background fluorescence. Experiments were performed in triplicate for each time point.

Biodistribution of C6 labeled, 4600-GRGDS nanospheres was also examined following the thrombogenic injury to the femoral artery. Nanospheres were injected intravenously through the femoral vein cannula. Organs were extracted one hour following or immediately after bleeding had stopped. Tissue was processed and C6 was quantified as described. Experiments were performed in triplicate at each time point.

Further analysis included the quantification of C6 associated with the clot following injury. Two groups were analyzed in the femoral artery injury, PEG 4600 and 4600-GRGDS nanospheres. Five rats were used in each group. Following injury and the cessation of bleeding, the clot was excised and immersed in acetonitrile (ACN) overnight. Samples were centrifuged and C6 content was determined with reverse-phase high performance liquid chromatography (HPLC) (Shimadzu Scientific Instruments) with a fluorescence detector and a Nova-Pak C18, 4 µm, 3.9mm × 150mm column (Waters). Mobile phase was prepared as described by Eley et al (19), and consisted of ACN:acetic acid (8%) (80:20 v/v) with a flow rate of 1.0 ml/minute. A standard curve for C6 (450/490nm (excitation/emission) and retention time ~ 3.1 minute) was established in ACN with a sensitivity limit of 0.25 ng/ml.

Clot visualization—In order to visualize C6 labeled nanospheres associated within clots following thrombogenic injury, injured vessel segments containing clots were excised and fixed in 10% formalin overnight. Following fixation, clots were either mounted for visualization via SEM, or embedded in OCT. Embedded clots were then cryo-sectioned to

15 μm cross-sections and mounted with Vector Shield with DAPI. Cross-sections were visualized with a Zeiss Axiovert 200 microscope (Carl Zeiss Inc.).

Statistical Analysis

Data were analyzed with a one-way analysis of variance (ANOVA) followed by the Student-Newman-Keuls test for determining differences between groups. Differences were accepted as statistically significant with $P < 0.05$. Student's t test was used for clot associated C6 comparison and in vitro assay validation with collagen.

One sentence summary

Synthetic platelets composed of functionalized nanoparticles halve bleeding time in a rat injury model and may prove useful in treating trauma victims.

Supplementary Material

Refer to Web version on PubMed Central for supplementary material.

Acknowledgments

None.

Funding: J.P.B. partially supported by the Coulter Foundation (Early Career Award to E.B.L.) and Richard and Gail Siegal. J.P.B. and R.R. partially supported by NIH Neuroengineering training grant T90-DK070068. C.A.W. partially supported by NIH MSTP training grant 5T32GM07025. C.A.W. and R.R. partially supported by Richard and Gail Siegal and Carol Sirot. S.S.S. supported by NIH grants HL56786 and HL41026.

References

1. Krug EG, Sharma GK, Lozano R. The global burden of injuries. *American Journal of Public Health* 2000;90:523. [PubMed: 10754963]
2. Champion HR, Bellamy RF, Roberts CP, Leppaniemi A. A profile of combat injury. *Journal of Trauma-Injury Infection and Critical Care* 2003;54:S13.
3. Sauaia A, Moore FA, Moore EE, Moser KS, Brennan R, Read RA, Pons PT. Epidemiology of trauma deaths- A reassessment. *Journal of Trauma-Injury Infection and Critical Care* 1995;38:185.
4. Regel G, Stalp M, Lehmann U, Seekamp A. Prehospital care, importance of early intervention on outcome. *Acta Anaesthesiol Scand Suppl* 1997;110:71. [PubMed: 9248540]
5. Kim HW, Greenburg AG. Toward 21st century blood component replacement therapeutics: Artificial oxygen carriers, platelet substitutes, recombinant clotting factors, and others. *Artificial Cells Blood Substitutes and Biotechnology* 2006;34:537.
6. Blajchman M. Substitutes for success. *Nature Medicine* 1999;5:17.
7. Boffard, KD.; Riou, B.; Warren, B.; Choong, PIT.; Rizoli, S.; Rossaint, R.; Axelsen, M.; Kluger, Y. 63rd Annual Meeting of the American-Association-for-the-Surgery-of-Trauma; Maui, HI. 2004; p. 8-16.
8. Benharash, P.; Bongard, F.; Putnam, B. Annual Meeting of the Southern California Chapter of the American-College-of-Surgeons; Southeastern Surgical Congress, Santa Barbara, CA. 2005; p. 776-780.
9. Lee DH, Blajchman MA. Novel treatment modalities: New platelet preparations and substitutes. *British Journal of Haematology* 2001;114:496. [PubMed: 11552973]
10. Ellis-Behnke RG, Liang YX, Tay DK, Kau PW, Schneider GE, Zhang S, Wu W, So KF. Nano hemostat solution: immediate hemostasis at the nanoscale. *Nanomedicine* 2006;2:207. [PubMed: 17292144]

11. Wong NS, Chang TM. Polyhemoglobin-fibrinogen: a novel oxygen carrier with platelet-like properties in a hemodiluted setting. *Artif Cells Blood Substit Immobil Biotechnol* 2007;35:481. [PubMed: 17922313]
12. Hans ML, Lowman AM. Biodegradable nanoparticles for drug delivery and targeting. *Current Opinion in Solid State & Materials Science* 2002;6:319.
13. Gref R, Luck M, Quellec P, Marchand M, Dellacherie E, Harnisch S, Blunk T, Muller RH. 'Stealth' corona-core nanoparticles surface modified by polyethylene glycol (PEG): influences of the corona (PEG chain length and surface density) and of the core composition on phagocytic uptake and plasma protein adsorption. *Colloids and Surfaces B-Biointerfaces* 2000;18:301.
14. Beer JH, Springer KT, Collier BS. Immobilized Arg-Gly-Asp (RGD) peptides of varying lengths as structural probes of the platelet glycoprotein-IIb/IIIa receptor. *Blood* 1992;79:117. [PubMed: 1728303]
15. Hirano Y, Okuno M, Hayashi T, Goto K, Nakajima A. Cell-attachment activities of surface immobilized oligopeptides RGD, RGDS, RGDV, RGDT, and YIGSR toward 5 cell-lines. *Journal of Biomaterials Science-Polymer Edition* 1993;4:235. [PubMed: 8476793]
16. Fuglsang J, Stender M, Zhou J, Moller J, Falk E, Ravn HB. Platelet activity and in vivo arterial thrombus formation in rats with mild hyperhomocysteinaemia. *Blood Coagulation & Fibrinolysis* 2002;13:683. [PubMed: 12441906]
17. Martinowitz U, Kenet G, Segal E, Luboshitz J, Lubetsky A, Ingerslev J, Lynn M. Recombinant activated factor VII for adjunctive hemorrhage control in trauma. *Journal of Trauma-Injury Infection and Critical Care* 2001;51:431.
18. Bell B, Canty D, Audet M. Hemophilia: an updated review. *Pediatr Rev* 1995;16:290. [PubMed: 7567698]
19. Eley JG, Pujari VD, McLane J. Poly (lactide-co-glycolide) nanoparticles containing coumarin-6 for suppository delivery: In vitro release profile and in vivo tissue distribution. *Drug Delivery* 2004;11:255. [PubMed: 15371107]
20. Chambers E, Mitragotri S. Long circulating nanoparticles via adhesion on red blood cells: Mechanism and extended circulation. *Experimental Biology and Medicine* 2007;232:958. [PubMed: 17609513]
21. Hersel U, Dahmen C, Kessler H. RGD modified polymers: biomaterials for stimulated cell adhesion and beyond. *Biomaterials* 2003;24:4385. [PubMed: 12922151]
22. Ebara M, Yamato M, Aoyagi T, Kikuchi A, Sakai K, Okano T. The effect of extensible PEG tethers on shielding between grafted thermo-responsive polymer chains and integrin-RGD binding. *Biomaterials* 2008;29:3650. [PubMed: 18582933]
23. Pytela R, Pierschbacher MD, Ginsberg MH, Plow EF, Ruoslahti E. Platelet Membrane Glycoprotein Iib/Iiia - Member of a Family of Arg-Gly-Asp Specific Adhesion Receptors. *Science* 1986;231:1559. [PubMed: 2420006]
24. Pierschbacher MD, Ruoslahti E. Influence of stereochemistry of the sequence Arg-Gly-Asp-Xaa on binding-specificity in cell-adhesion. *Journal of Biological Chemistry* 1987;262:17294. [PubMed: 3693352]
25. Pierschbacher MD, Ruoslahti E. Cell attachment activity of fibronectin can be duplicated by small synthetic fragments of the molecule. *Nature* 1984;309:30. [PubMed: 6325925]
26. Boxus T, Touillaux R, Dive G, Marchand-Brynaert J. Synthesis and evaluation of RGD peptidomimetics aimed at surface bioderivatization of polymer substrates. *Bioorganic & Medicinal Chemistry* 1998;6:1577. [PubMed: 9801829]
27. Radomski A, Jurasz P, Alonso-Escolano D, Drews M, Morandi M, Malinski T, Radomski MW. Nanoparticle-induced platelet aggregation and vascular thrombosis. *British Journal of Pharmacology* 2005;146:882. [PubMed: 16158070]
28. Sahli H, TaponBretaudiere J, Fischer AM, Sternberg C, Spenlehauer G, Verrecchia T, Labarre D. Interactions of poly(lactic acid) and poly(lactic acid-co-ethylene oxide) nanoparticles with the plasma factors of the coagulation system. *Biomaterials* 1997;18:281. [PubMed: 9068888]
29. Chang TM, Powanda D, Yu WP. Analysis of polyethylene-glycol-poly(lactide) nano-dimension artificial red blood cells in maintaining systemic hemoglobin levels and prevention of

- methemoglobin formation. *Artif Cells Blood Substit Immobil Biotechnol* 2003;31:231. [PubMed: 12906306]
30. Jain RA. The manufacturing techniques of various drug loaded biodegradable poly(lactide-co-glycolide) (PLGA) devices. *Biomaterials* 2000;21:2475. [PubMed: 11055295]
 31. Harris JM. Laboratory synthesis of polyethylene-glycol derivatives. *Journal of Macromolecular Science-Reviews in Macromolecular Chemistry and Physics* 1985;C25:325.
 32. Kleiman NS, Lincoff AM, Flaker GC, Pieper KS, Wilcox RG, Berdan LG, Lorenz TJ, Cokkinos DV, Simoons ML, Boersma E, Topol EJ, Califf RM, Harrington RA, P. Investigators. Early percutaneous coronary intervention, platelet inhibition with eptifibatid, and clinical outcomes in patients with acute coronary syndromes. *Circulation* 2000;101:751. [PubMed: 10683348]
 33. Klibanov AL, Maruyama K, Torchilin VP, Huang L. Amphipathic polyethyleneglycols effectively prolong the circulation time of liposomes. *Febs Letters* 1990;268:235. [PubMed: 2384160]
 34. Deng C, Chen X, Yu H, Sun J, Lu T, Jing X. A biodegradable triblock copolymer poly(ethylene glycol)-b-poly(L-lactide)-b-poly(L-lysine): Synthesis, self-assembly, and RGD peptide modification. *Polymer* 2007;48:139.
 35. Coller BS, Springer KT, Beer JH, Mohandas N, Scudder LE, Norton KJ, West SM. Thromboerythrocytes - Invitro Studies of a Potential Autologous, Semiartificial Alternative to Platelet Transfusions. *Journal of Clinical Investigation* 1992;89:546. [PubMed: 1737845]

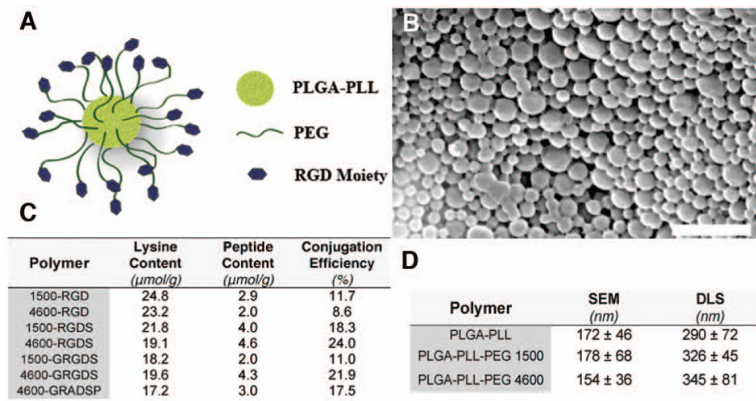


Fig. 1. Design, synthesis and characterization of synthetic platelets. (A) Schematic of synthetic platelet comprised of PLGA-PLL core with PEG arms terminated with the RGD moiety. (B) Scanning electron microscope (SEM) micrograph of synthetic platelets. Scale bar, 1 μm . (C) Lysine and peptide concentrations of synthetic platelets as determined by amino acid analysis. Conjugation efficiency was defined as the peptide to lysine ratio multiplied by 100. (D) Diameter of PLGA-PLL core and PLGA-PLL-PEG nanospheres as determined by SEM microscopy and dynamic light scattering (DLS). SEM diameter based on $n = 80$. Data are expressed as mean \pm SD.

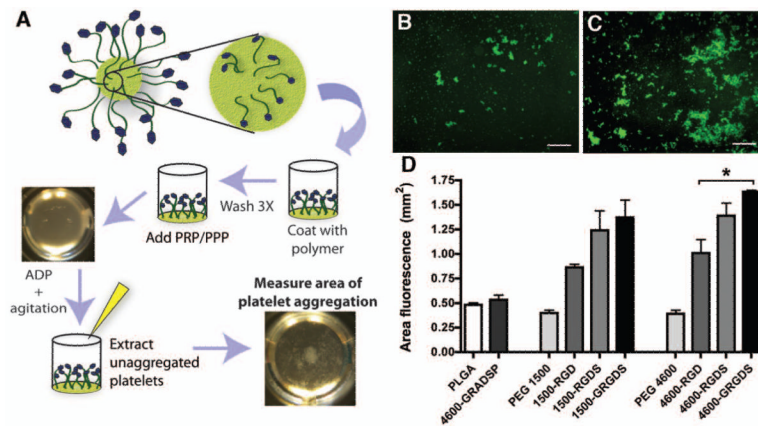
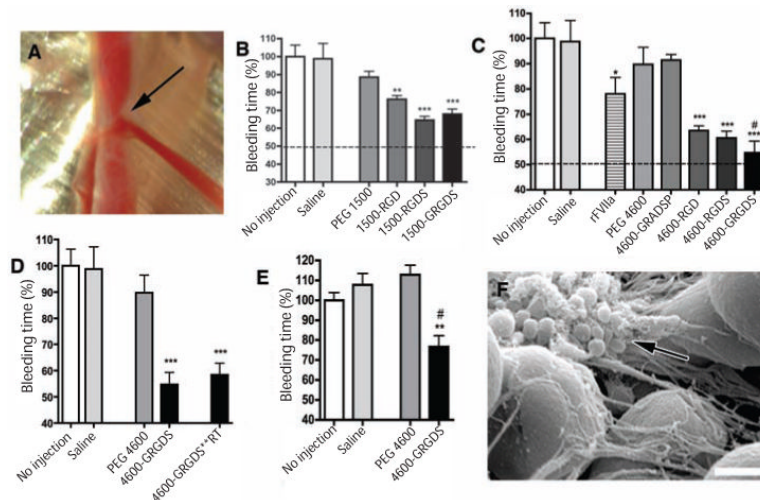


Fig. 2.

In vitro characterization of the interactions of polymers with activated platelets. (A) Schematic of in vitro assay for quantifying platelet adhesion to polymers. Adhesion of 5-chloromethylfluorescein diacetate (CMFDA)-labeled platelets to polymers after agitation and addition of ADP. Appearance of assay with (B) PEG 4600 and (C) 4600-GRGDS. Scale bar, 500 µm. (D) Quantification of platelet adhesion. Area of fluorescence represents area of platelet aggregation (n = 3). Data are expressed as mean ± SEM. * significant at P < 0.05 compared to PEG 4600 alone.

**Fig. 3.**

In vivo performance of synthetic platelets: hemostatic efficacy. (A) Femoral artery injury model used for all studies. Arrow, injury site and the blood spurting from the injured vessel. (B) Bleeding times following intravenous administration of PEG 1500 synthetic platelets at 20 mg/ml ($n = 5$). Data are presented as percentage of no injection mean value \pm SEM. ** $P < 0.01$ and *** $P < 0.001$ significant as compared to PEG 1500 alone. (C) Bleeding times after intravenous administration of PEG 4600 synthetic platelets at 20 mg/ml and rFVIIa at 100 μ g/kg ($n = 5$). Data are presented as percentage of no injection mean value \pm SEM. * $P < 0.05$ and *** $P < 0.001$ compared to saline, and # $P < 0.05$ compared to rFVIIa. (D) Bleeding times comparing synthetic platelet administration, PEG-4600-GRGDS, to synthetic platelets stored in a lyophilized state at room temperature for two weeks, 4600-GRGDS**RT ($n=5$). Data are presented as percentage of no injection mean value \pm SEM. *** $P < 0.001$ compared to PEG 4600 alone. (E) Bleeding times when treatments were administered after injury. Bleeding times represented as a percentage of no injection bleeding time values (255 ± 12 seconds). Synthetic platelets were administered at 20 mg/ml. Data are presented as mean \pm SEM ($n = 5$). ** $P < 0.01$ compared to saline injection and # $P < 0.01$ compared to no injection. (F) SEM micrograph of clot excised from injured artery after synthetic platelet administration (4600-GRGDS). Synthetic platelets intimately associated with clot and connecting fibrin mesh (arrow) The large (5 μ m) spheres are blood cells. Scale bar, 1 μ m.

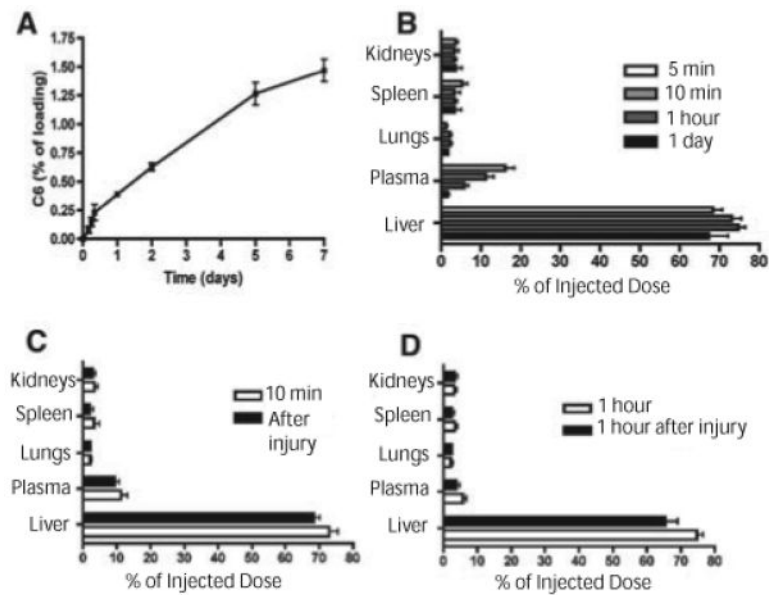


Fig. 4. Biodistribution of 4600-GRGDS synthetic platelets. (A) In vitro evaluation of cumulative C6 released from C6 loaded synthetic platelets over 7 days. Data are presented as mean \pm SD ($n = 3$). (B) Biodistribution of 4600-GRGDS synthetic platelets. No fluorescence was detected at 3 and 7 day time points following injection ($n = 3$). Data are expressed as mean \pm SEM. (C) Biodistribution of 4600-GRGDS synthetic platelets (20 mg/ml injection dose) immediately following femoral artery injury ($n = 3$). Because synthetic platelets are allowed to circulate for 5 minutes prior to injury, and the injury bleeds for approximately 3 minutes, this time is compared to 10 minute biodistribution with no injury. Data are presented as mean \pm SEM (D) Biodistribution of 4600-GRGDS synthetic platelets 1 hour following femoral artery injury ($n = 3$). Data are presented as mean \pm SEM. In all cases, synthetic platelets were administered at 20 mg/ml in 0.5 ml of Ringer's Saline Solution.

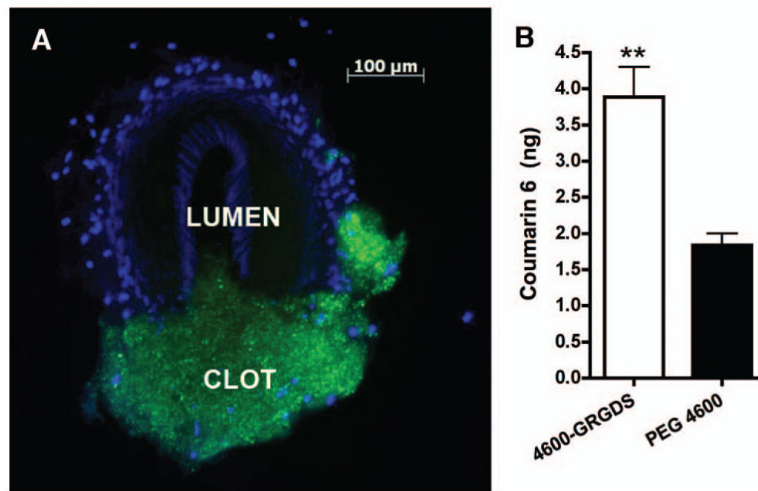


Fig. 5. Coumarin-6 visualization and quantification of synthetic platelets. (A) Cross-section of clot after femoral artery injury and injection of C6 labeled synthetic platelets. Blue, DAPI-labeled nuclei of smooth muscle and endothelial cells; green, C6 from synthetic platelets within clot. Scale bar, 100 μ m. (B) HPLC quantification of clot-associated C6 following injury (n = 5). Data are expressed as mean \pm SEM (** P < 0.01).